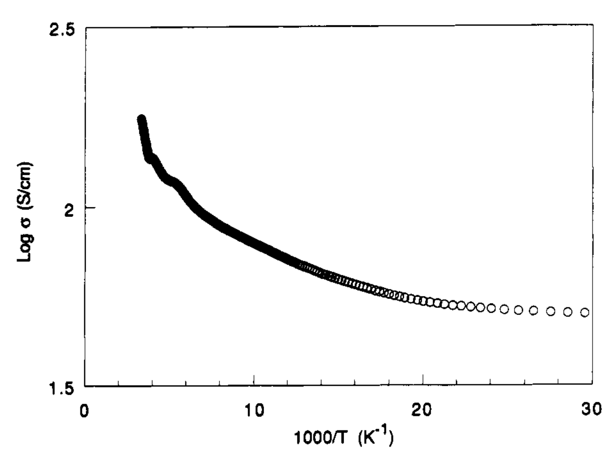

Figure 4. Four-probe electrical conductivity data as a function of temperature for a single crystal of $K_4Cu_8Te_{11}$.

compound. Selected bond distances and angles are shown in Figure 3.

There are four crystallographically distinct K atoms in this compound. The encapsulated K(1) atom is sitting slightly off-center in a rectangular plane defined by two opposite parallel ditellurides in the dodecahedral cluster. K–Te distances range from 3.676 (3) Å to 3.960 (3) Å (average of 3.75 (8) Å), and Cu–K distances range from 3.674 (3) Å to 3.724 (3) Å (average of 3.69 (7) Å). The remaining three K atoms are sitting in the tunnels with various coordination environments {8 C.N. for K(2), 10 C.N. for K(3), 6 C.N. for K(4)}. The average K–Te distances are 3.70 (16) Å for K(2), 3.66 (23) Å for K(3), and 3.71 (9) Å for K(4).

If the formal charges on the ditelluride units and monotelluride atoms are considered as −2, each Cu atoms has a formal oxidation state of +1. This suggests that $K_4Cu_8Te_{11}$ would be a semiconductor. Preliminary conductivity measurements on single crystals show a thermally activated behavior, as shown in Figure 4. However the strong deviation from linearity of the log σ vs. $1/T$ plot suggests a departure from classical semiconductor charge transport. The room-temperature conductivity is relatively high at ~160 S/cm.

The 20-vertex dodecahedral $Cu_8(Te_2)_6$ cluster and 16-vertex Cu_8Te_8 cluster are unique and, to the best of our knowledge, have no analogues in metal cluster chemistry. However, there is one 20-vertex dodecahedral cluster known, in organic chemistry, the dodecahedrane $C_{20}H_{20}$.[12] It is possible that the driving force for the stabilization of $Cu_8(Te_2)_6$ cluster is the encapsulation of the K ion. One could envision the possibility of building up novel extended structures in two or three dimensions based on this dodecahedral $Cu_8(Te_2)_6$ cluster by sharing more or all the ditelluride edges. We are expecting more of this structural motif in the Cu/Te system and further explorations with A_2Te_x/Cu suggest that this is indeed the case.[13]

Acknowledgment. Financial support from the National Science Foundation for a Presidential Young Investigator Award, CHE-8958451, is gratefully acknowledged. The X-ray instrumentation used in this work was purchased in part with funds from the National Science Foundation (CHE-8908088). We thank Don C. DeGroot for electrical conductivity measurements. This work made use of the SEM facilities of the Center for Electron Optics at Michigan State University.

Supplementary Material Available: Tables of atomic coordinates of all atoms and anisotropic and isotropic thermal parameters of all non-hydrogen atoms, bond distances and angles, and calculated and observed X-ray powder diffraction patterns (21 pages); a listing of calculated and observed ($10F_o/10F_c$) structure factors (15 pages). Ordering information is given on any current masthead page.

---

(12) Ternansky, R. J.; Balogh, D. W.; Paquette, L. A. *J. Am. Chem. Soc.* **1982**, *104*, 4503–4504.

(13) Park, Y.; Kanatzidis, M. G., to be published.

Dynamic Atomic-Level Observation of Staging Phenomena in Silver and Mercury Intercalates of Titanium Disulfide

M. McKelvy,*,[†] R. Sharma,[†] E. Ong,[‡] G. Burr,[§] and W. Glaunsinger[§]

Center for Solid State Science
Arizona State University, Tempe, Arizona 85287-1704
Manuel Lujan, Jr. Neutron Scattering Center
MS-H805, Los Alamos National Laboratory
Los Alamos, New Mexico 87545
Department of Chemistry, Arizona State University
Tempe, Arizona 85287-1604

Received May 7, 1991
Revised Manuscript Received July 29, 1991

Intercalation can be used to tailor the chemical and physical properties of layered compounds, resulting in a complete range of property modifications from subtle to extreme and compounds with important applications.[1–8] A general feature associated with property modifications and many applications is the effective dimensionality of the host. In this regard, staging is of fundamental significance.[6,8–10]

The phenomenon of staging is certainly one of the most extraordinary structural properties of intercalation compounds. Stage-*n* intercalates characteristically have *n* host layers between guest layers. These structures are generally found in hosts with relatively thin, flexible layers, such as the transition-metal dichalcogenides (TMDs) and graphite, which enhance both the elastic and electrostatic interlayer repulsive forces associated with staging.[8] Although staging has been the subject of numerous theoretical and experimental studies, it remains one of the most important and controversial subjects in this field.[6,8,11–14] A key question of current interest involves the roles of thermodynamics and kinetics in the staging process.

Substantial evidence indicates that observed stage

[†] Center for Solid State Science, Arizona State University.

[‡] Los Alamos National Laboratory.

[§] Department of Chemistry, Arizona State University.

* To whom correspondence should be addressed.

(1) Levy, F., Ed. *Intercalated Layered Materials*; D. Reidel: Dordrecht, Holland, 1979.

(2) Whittingham, M. S., Jacobson, A. J., Eds. *Intercalation Chemistry*; Academic Press: New York, 1982.

(3) Dresselhaus, M. S., Dresselhaus, G., Fischer, J. E., Moran, M. J., Eds. *Intercalated Graphite*; North-Holland: New York, 1983.

(4) Atwood, J. L., Davies, J. E. D., MacNicol, D. D., Eds. *Inclusion Compounds*; Academic Press: London, 1984.

(5) Dresselhaus, M. S., Ed. *Intercalation in Layered Materials*; Plenum Press: New York, 986.

(6) Ulloa, S. E.; Kirczenow, G. *Comments Cond. Mat. Phys.* **1986**, *12*, 181–197.

(7) Legrand, A. P.; Flandrois, S., Eds. *Chemical Physics of Intercalation*; Plenum Press: New York, 1987.

(8) Safran, S. A. *Solid State Phys.* **1987**, *40*, 183–246.

(9) Safran, S. A. In ref 7, pp 47–57.

(10) Fischer, J. E. In ref 7, pp 59–78.

(11) Miyazaki, H. *J. Mater. Res.* **1988**, *3*, 479–490.

(12) Suematsu, H.; Suda, K.; Metoki, N. *Synth. Met.* **1988**, *23*, 7–12.

(13) Kirczenow, G. *Synth. Met.* **1988**, *23*, 1–6.

(14) Cajipe, V.; Heiney, P. A.; Fischer, J. E. *Phys. Rev. B* **1989**, *39*, 4374–4385.

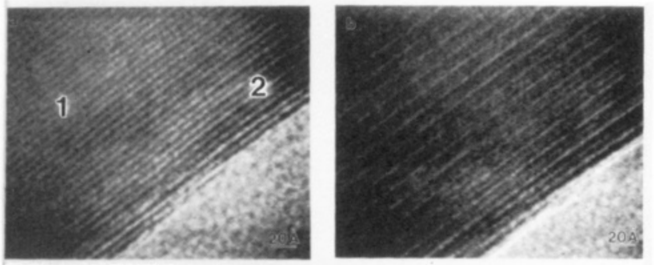

Figure 1. $Ag_{0.17}TiS_2$: (a) primarily stage 1 with a small region of intergrown stage 2; (b) same region after the stage-1 to stage-2 transition induced by electron beam heating. Note: Neighboring layers in the stage-1 region in (a) have essentially the same repeat distance (6.0 Å) when measurements are averaged over dozens of locations, whereas neighboring layers in (b) have alternating average layer spacings, where observable, of 5.7 and 6.3 Å, consistent with the ambient-temperature structure of stage-2 $Ag_{0.17}TiS_2$.

transformations are associated with the intralayer motion of guest islands.[6,8,9,15] In the Daumas–Hérold (DH) model, the islands are staged along the layer stacking (*c*) axis, with large numbers of islands and similar guest concentrations in each van der Waals gap.[16] Island size and concentration can dramatically affect material properties, with available evidence indicating island sizes can range from ~100 Å to macroscopic dimensions.[6,17,18] The presence of DH islands demonstrates the importance of kinetics, since, in the thermodynamic limit, minimization of host-layer strain should result in macroscopic guest layers.[8,9]

The most direct evidence for staged structures and models has come from atomic-scale observations using high-resolution transmission electron microscopy (HRTEM). Several HRTEM studies have revealed large, coherent stage-*n* regions, staging disorder, mixed staging, and guest islands and dislocations.[6,17-20] In contrast to these static observations, the potential of dynamic HRTEM (DHRTEM) to explore the staging process at the atomic level is virtually untapped.[21]

This study summarizes our initial efforts to use the unique capabilities of DHRTEM to provide previously unavailable dynamic atomic-level insight into staging processes. Herein, we report the first DHRTEM investigations of the staging mechanisms associated with model ionic, $Ag^{+}_{0.17}TiS_2^{0.17-}$, and neutral, $Hg^{0}_{x}TiS_2$ ($1.25 \geq x \geq 0.00$), intercalates.[23,24] These model systems were chosen since they allow the study of staging processes in the presence and absence of interlayer guest–guest electrostatic repulsions, respectively. This, in turn, allows atomic-level evaluation of the relative importance of elastic and electrostatic forces to staging processes. This comparison of model systems became possible with the recent discovery of the unique, essentially neutral nature of Hg in Hg_xTiS_2[24]. Many observations, including the lack of Li^+ ion exchange, essentially no sulfur radius change upon intercalation, the ability of ammonia to reduce Hg_xTiS_2, and random staging for $x \ll 1.25$ indicate a lack of charge transfer. However, the possibility of a small amount of covalent electron exchange cannot be ruled out based on these studies.[24]

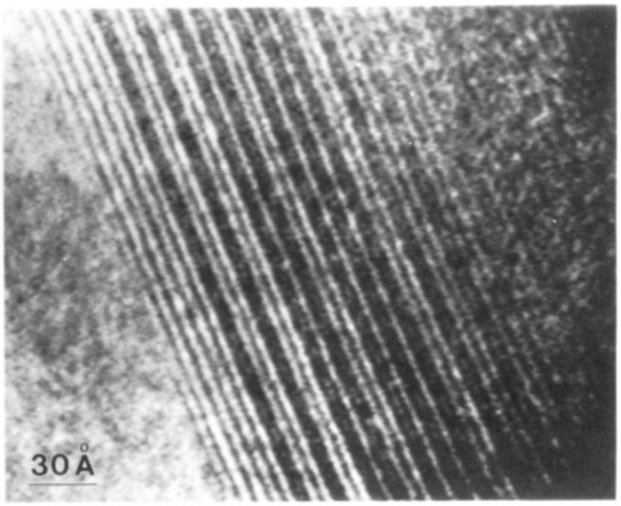

Figure 2. Randomly staged Hg_xTiS_2 obtained by the partial Hg deintercalation associated with warming stage-1 $Hg_{1.25}TiS_2$ from −170 °C to ambient temperature in the microscope vacuum. Note the preferential deintercalation near the external basal plane. The broad and narrow dark layers correspond to the intercalated (8.7-Å interlayer spacing) and empty (5.7-Å interlayer spacing) host layers, respectively.

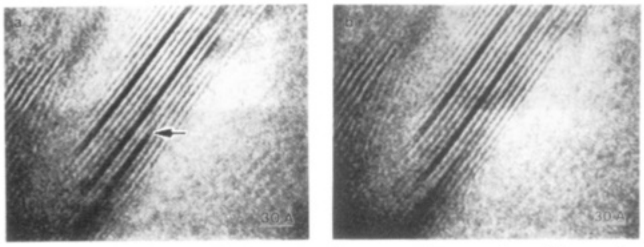

Figure 3. Deintercalation of a Hg guest–layer edge dislocation in Hg_xTiS_2 ($x \ll 1.25$): (a) before deintercalation, "squirting out", to the lower left; (b) after deintercalation.

Stage-2 $Ag_{0.17}TiS_2$ was prepared by reacting Ag and highly stoichiometric TiS_2 ($Ti_{1.002}S_2$) in sealed quartz ampules at 800 °C, followed by slow cooling to ambient temperature.[23] $Ag_{0.17}TiS_2$ undergoes a transition to stage 1 upon heating to 850–1050 °C. By quenching the stage-1 material to ambient temperature, it was trapped in metastable form, along with the formation of some stage-2 material.[23] Stage-1 $Hg_{1.25}TiS_2$ was prepared by direct reaction of Hg with highly stoichiometric TiS_2 in sealed quartz ampules at 300 °C, followed by slow cooling to ambient temperature.[24]

Specimens for DHRTEM study were crushed in an agate mortar and pestle under liquid nitrogen in a nitrogen cabinet. X-ray powder diffraction (XPD) verified the absence of significant structural change during crushing. These studies were performed on JEOL 4000 EX (1.7-Å point-to-point resolution) and JEOL 2000 FX (2.5-Å point-to-point resolution) electron microscopes coupled with 30 frame/s video recording systems. The still images in Figures 1–4 are taken from videotape.

The metastable stage-1 and stage-2 forms of quenched $Ag_{0.17}TiS_2$ identified by XPD were routinely observed by

---

(15) Solin, S. A. *Adv. Chem. Phys.* **1982**, *49*, 455–532.

(16) Daumas, N.; Hérold, A. *C. R. Seances Acad. Sci., Ser. C* **1969**, *268*, 373–375.

(17) Timp, G.; Dresselhaus, M. S. *J. Phys. C.* **1984**, *17*, 2641–2651.

(18) Dresselhaus, M. S.; Speck, J. S. In ref 5, pp 213–228.

(19) Thomas, J. M.; Millward, G. R.; Schlogl, R. F.; Boehm, H. P. *Mater. Res. Bull.* **1975**, *15*, 671–676.

(20) Dorignac, D.; Lahana, M. J.; Jagut, R.; Jouffrey, B.; Flandrois, S.; Hauw, C. *Mater. Res. Soc. Symp. Proc.* **983**, *20*, 33–38.

(21) J. M. Thomas previously reported a DHRTEM staging investigation of alkylamine TMDICs at the Chemical Society's Tilden Symposium (Scientific Societies Meeting Place, Savile Row, London, September 1973). However, these studies have not been published. The compounds investigated are best considered as redox-rearrangement intercalates, containing both neutral and ionic guest species resulting from redox reactions accompanying the intercalation process.[22]

(22) McKelvy, M. J.; Glaunsinger, W. S. *Annu. Rev. Phys. Chem.* **1990**, *41*, 497–523.

(23) Burr, G. L.; Young, Jr., V. G.; McKelvy, M. J.; Glaunsinger, W. S.; Von Dreele, R. B. *J. Solid State Chem.* **1990**, *84*, 355–364.

(24) Ong, E. W.; McKelvy, M. J.; Ouvrard, G.; Glaunsinger, W. S. *Chem. Mater.*, in press.

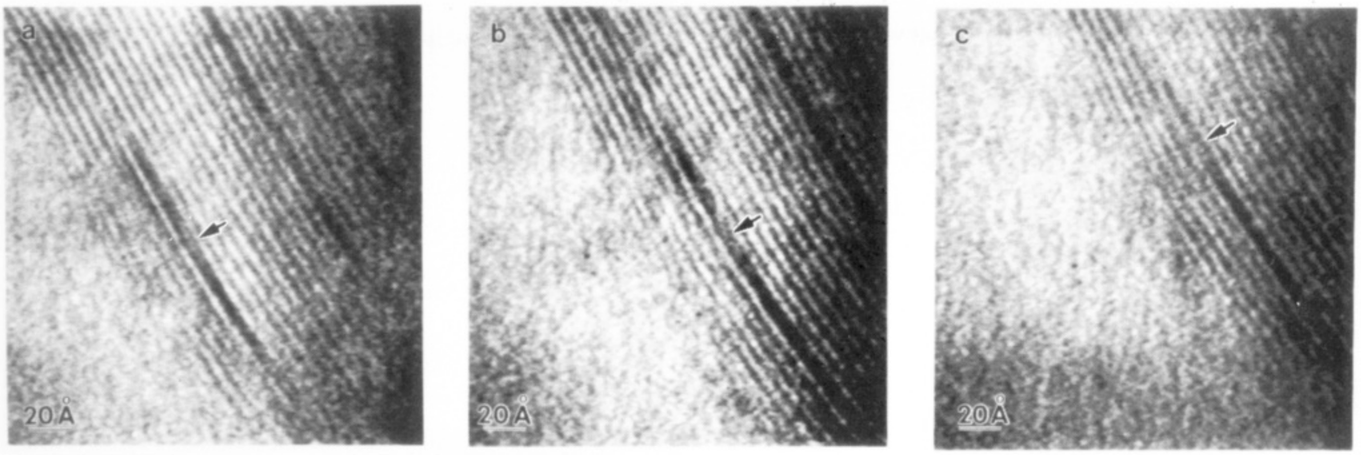

Figure 4. Hg island separation and deintercalation from a guest–layer edge dislocation in Hg_xTiS_2 ($x \ll 1.25$): (a) initiation; (b) island separation showing a slight host layer expansion around the island; (c) after island deintercalation is essentially complete. Note: The small black arrow indicates the island-separation region and its position is constant for reference.

HRTEM. The layer spacings determined by HRTEM and XPD were the same within experimental error (c = 5.90–5.98 ± 0.06 Å and 11.94–12.16 ± 0.12 Å for stages 1 and 2, respectively). The intrastage variations in c are likely due to incomplete quenching.

We successfully induced the metastable stage-1 to stage-2 transition during DHRTEM study by electron-beam heating. A small stage-2 region was initially observed in a primarily stage-1 crystallite (Figure 1a). Upon heating, the transition appeared to proceed by the advance of a somewhat irregular stage-2/stage-1 interface, eventually yielding a stage-2 crystallite (Figure 1b). This observation is consistent with stage-n and stage-($n - 1$) regions separated by a narrow, possibly disordered, boundary region, as observed macroscopically during H_2SO_4–graphite intercalation,[25,26] rather than a continuous stage-disordered transition.[13]

$Hg_{1.25}TiS_2$ was observed by DHRTEM at −170 °C to be stage-1 with an 8.7-Å layer repeat, which is experimentally equivalent to the 8.68-Å stage-1 layer spacing observed at ambient temperature by XPD.[24] Warming the sample to ambient temperature in the microscope vacuum results in substantial Hg deintercalation and a randomly staged structure (Figure 2), consistent with XPD studies of Hg_xTiS_2 for $x \ll 1.25$.[24] Preferential deintercalation of the layers nearest the external basal planes often occurs (Figure 2). This may be due to their greater flexibility and suggests these layers are generally more reactive and associated with the onset of deintercalation. Previous work by Hooley et al. also indicates that bromine intercalation of graphite is initiated at the external basal planes,[27] suggesting these planes are generally more reactive during both intercalation and deintercalation processes.

Further Hg deintercalation was induced by electron beam heating. This also ocurred in a generally random fashion but with a preference for deintercalation of guest layers neighboring occupied host layers, indicating the possible presence of weak residual elastic interlayer repulsive interactions associated with the discrete size of the Hg atoms.[8]

Two mechanisms were observed for deintercalation associated with guest–layer dislocations: (1) deintercalation of the Hg dislocation away from its termination, indicating the elastic strain at the termination is essentially "squeezing out" the dislocation (Figure 3); (2) intercalant island separation from the end of a dislocation and its subsequent deintercalation (Figure 4). The latter observation is somewhat unexpected and may be due to the presence of 0.2% excess Ti^{4+} in the guest layer,[28] which could pull the host layers together at the separation site and induce island separation. This could provide sufficient strain on both sides of the island to force its deintercalation parallel to the electron beam. This mechanism is consistent with the slight layer expansion that appears to occur around the island while it is being "pinched" off (Figure 4b). Such an expansion may be necessary locally to allow Hg to escape parallel to the electron beam.

The different types of staging behavior observed for $Ag^{+}_{0.17}TiS_2^{0.17-}$ and $Hg^0_xTiS_2$ can be directly related to their ionic and essentially neutral guest species, respectively. In the former compound, significant interlayer guest–guest electrostatic repulsions result in long range stage-2 ordering. However, in the latter compound, such repulsions are basically absent due to the essentially neutral nature of Hg[24] resulting in very weak interlayer repulsive forces and random staging. The above observations underscore the importance of interlayer electrostatic repulsions to stage ordering and suggest they can independently induce stage ordering for ionic TMD intercalation compounds (TMDICs). These observations also suggest residual elastic repulsions play a relatively minor role in stage ordering for ionic TMDICs.[8]

By DHRTEM observation of model ionic and neutral TMDICs, it is possible to begin to probe the mechanisms of and forces responsible for staging at the atomic level. These initial observations indicate (1) electrostatic interlayer guest–guest repulsions can induce stage ordering, (2) residual elastic repulsions apparently have relatively little effect on stage ordering for TMDICs, (3) the layers nearest the external basal planes deintercalate preferentially, suggesting they are generally more reactive, and (4) host–layer pinning associated with excess TM in the guest layers may result in new transition mechanisms. Investigations, primarily perpendicular to the Hg_xTiS_2 layers, are currently underway to better elucidate the role of intercalant domains/islands.

It is apparent from the present investigation that DHRTEM provides a unique and powerful tool for real-time observation of staging transitions as well as evaluating

---

(25) Nishitani, R.; Sasaki, Y.; Nishina, Y. *J. Phys. Soc. Jpn.* **1987**, *56*, 1051–1057.

(26) Nishitani, R.; Sasaki, Y.; Nishina, Y. *Synth. Met.* **1989**, *34*, 315–321.

(27) Hooley, J. *Mater. Sci. Eng.* **1977**, *31*, 17–24; *Carbon* **1980**, *18*, 82–92.

(28) McKelvy, M. J.; Glaunsinger, W. S. *J. Solid State Chem.* **1987**, *66*, 181–188.

theoretical models at the atomic level. Such studies should complement the results obtained from recent staging-kinetics studies (e.g., Raman, optical and X-ray/neutron diffraction).[8,14,25,26,29] A full account of our DHRTEM studies of staging mechanisms will be published in the near future.

Acknowledgment. We are grateful for the use of the National Science Foundation (DMR 8913384)/Arizona State University High Resolution Electron Microscopy and the Center for Solid State Science Materials Preparation Facilities. We also thank the Department of Chemistry for the use of its X-ray Facility and Glass Shop and Dr. G. Ouvrard for preparing the $Hg_{1.25}TiS_2$ samples and helpful discussions.

---

(29) Okabe, K.; Tanuma, S. *Synth. Met.* **1988**, *23*, 61–66.

Ultraviolet Radiation-Induced Cross-Linking of Poly[bis(2-(2-methoxyethoxy)ethoxy)phosphazene]

Constance J. Nelson, William D. Coggio, and
Harry R. Allcock*

Department of Chemistry
The Pennsylvania State University
University Park, Pennsylvania 16802

Received June 21, 1991
Revised Manuscript Received August 13, 1991

An increasing interest is evident in the design and development of conductive polymeric electrolytes for the possible fabrication of solid-state batteries.[1] It has been shown previously that poly[bis(2-(2-methoxyethoxy)ethoxy)phosphazene] (1) possesses an ambient temperature ionic conductivity 2–3 orders of magnitude higher than poly(ethylene oxide), when each system is complexed with $LiCF_3SO_3$.[2-6]

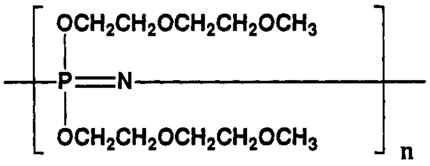

$$\left[-\underset{OCH_2CH_2OCH_2CH_2OCH_3}{\overset{OCH_2CH_2OCH_2CH_2OCH_3}{P}}{=}N- \right]_n$$

1

However, a problem associated with the practical application of this polymer is its tendency to flow under light pressure. A method that has been employed successfully to increase the dimensional stability is the use of cross-linking. It has been shown that 1 can be cross-linked both chemically and by use of ^{60}Co γ-irradiation.[7-9] Recently, Abraham and co-workers reported another technique that utilizes $LiAlCl_4$ to form a stabilized complex with polymer 1.[10]

Scheme I

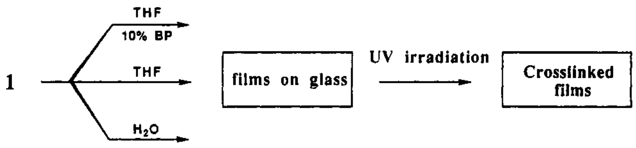

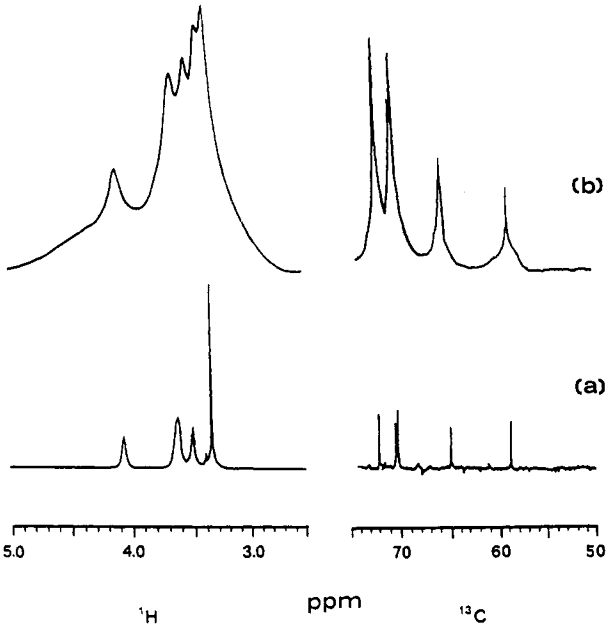

Figure 1. The 360-MHz ^{1}H and ^{13}C NMR spectra in $CDCl_3$ of (a) polymer 1 and (b) the swollen gel of cross-linked polymer 1.

Chemical cross-linking requires the incorporation of a difunctional reagent, thus introducing impurities into the system. ^{60}Co γ-irradiation is a much cleaner method, but its limited accessibility and related expense make use of this technique less attractive.

We report here that ultraviolet radiation can be used to cross-link polymer 1. This method offers advantages in that it allows efficient cross-linking of 1 via an inexpensive, readily available ultraviolet radiation source and yields a pure product.

The polymer 1 utilized in this study was synthesized via published methods.[2,5,11] In a typical reaction 1 was dissolved in tetrahydrofuran with 10 mol % benzophenone added as the photoinitiator. This mixture was then solution-cast as a film on glass, and the solvent was allowed to evaporate. The polymer-coated glass slides were then placed in quartz reaction tubes, which were purged with argon, sealed, and irradiated for 20 min with a 450-W Hg lamp.[12] The cross-linked films were then purified by

---

(1) Shriver, D. F.; Farrington, G. C. *Chem. Eng. News* **1985**, *63*(20), 42.

(2) Blonsky, P. M.; Shriver, D. F.; Austin, P. E.; Allcock, H. R. *J. Am. Chem. Soc.* **1984**, *106*, 6854.

(3) Blonsky, P. M.; Shriver, D. F.; Austin, P.; Allcock, H. R. *Polym. Mater. Sci. Eng.* **1985**, *53*, 118.

(4) Blonsky, P. M.; Shriver, D. F.; Austin, P.; Allcock, H. R. *Solid State Ionics* **1986**, *18/19*, 258.

(5) Allcock, H. R.; Austin, P. E.; Neenan, T. X.; Sisko, J. T.; Blonsky, P. M.; Shriver, D. F. *Macromolecules* **1986**, *19*, 1508.

(6) Bennett, J. L.; Dembek, A. A.; Allcock, H. R.; Heyen, B. J.; Shriver, D. F. *Chem. Mater.* **1989**, *1*, 14.

(7) Tonge, J. S.; Shriver, D. F. *J. Electrochem. Soc.* **1987**, *134*, 269.

(8) Allcock, H. R.; Kwon, S.; Riding, G. H.; Fitzpatrick, R. J.; Bennett, J. L. *Biomaterials* **1988**, *9*, 509.

(9) Allcock, H. R.; Fitzpatrick, R. J.; Gebura, M.; Kwon, S. *Polym. Prepr.* (*Am. Chem. Soc., Div. Polym. Chem.*) **1987**, *28* (1), 321.

(10) Abraham, K. M.; Alamgir, M. *Chem. Mater.* **1991**, *3*, 339.

(11) Polymer 1 was characterized by ^{1}H NMR ($CDCl_3$): OCH_2CH_2 4.1 ppm; CH_2OCH_2 3.65 ppm; CH_2OCH_3 3.57 ppm; CH_3 3.38 ppm. ^{13}C NMR: OCH_2CH_2 72.0, 70.3 ppm; OCH_2CH_2 70.4, 65.0 ppm; OCH_3 58.8 ppm. ^{31}P NMR: $\delta = -8.4$ (s). GPC: $M_w = 4 \times 10^5$, $M_n = 2 \times 10^5$. DSC: $T_g = -84.4$ °C. Anal. Calcd: C, 42.40; H, 7.83; N, 4.94; Cl, 0.00. Found: C, 42.99; H, 7.77; N, 4.43; Cl, 0.02.

(12) A Canrad-Hanovia medium-pressure, quartz, mercury vapor lamp equipped with a water-cooled quartz immersion well was utilized. The typical emitted ultraviolet radiation for this system is between 220 and 400 nm. The samples were irradiated in quartz reaction tubes which were placed in a rotating carousel at an approximate distance of 7 cm from the unfiltered source.

0897-4756/91/2803-0786$02.50/0